ISSN 1062-8738, Bulletin of the Russian Academy of Sciences: Physics, 2023, Vol. 87, No. 6, pp. 710–714. © Allerton Press, Inc., 2023.
Russian Text © The Author(s), 2023, published in Izvestiya Rossiiskoi Akademii Nauk, Seriya Fizicheskaya, 2023, Vol. 87, No. 6, pp. 807–812.

Fabrication of Optical Microstructures with Gradient Refractive Index by Two-Photon Laser Lithography

M. D. Aparin[a], *, T. G. Baluyan[a], M. I. Sharipova[a], M. A. Sirotin[a], E. V. Lyubin[a], I. V. Soboleva[a], V. O. Bessonov[a], and A. A. Fedyanin[a]

[a] *Department of Physics, Moscow State University, Moscow, 119991 Russia*

**e-mail: aparin@nanolab.phys.msu.ru*

Received December 5, 2022; revised December 23, 2022; accepted February 27, 2023

Abstract—The method of two-photon lithography is used to fabricate microstructures with gradient of refractive index. The rectangular structures with sizes 25 × 25 × 3 μm were fabricated with varying laser intensity by linear or Gaussian distribution in one dimension. The resulting refractive index has been tuned in the range of 0.03. The suggested method can be applied to produce arbitrarily shaped 3D GRIN micro-optical elements.

DOI: 10.3103/S1062873823701976

INTRODUCTION

Gradient, or GRIN (gradient index), optics, is a branch of optics that studies light propagation characteristics in optically inhomogeneous media with spatial variation of refractive index [1]. In gradient index materials, in contrast to homogeneous ones, the trajectories of the light rays are curved due to a variable refractive index. Such materials allow one to create optical elements with arbitrary surface shape, which can be used in fiber optic communication and imaging systems [2, 3], as well as in optical medical devices [4]. GRIN optical elements can be fabricated by several methods, including chemical vapor deposition [5], ion exchange [6], neutron irradiation [7], thermal sputtering [8] and photolithography [9, 10]. Despite the diversity of these methods, all of them are limited in the ability to produce three-dimensional objects of arbitrary shape, especially when it comes down to the microscale. There are methods for printing three-dimensional gradient optical elements; however, these are mostly macro-objects with characteristic dimensions in the order of centimeters and a resolution of fractions of a millimeter [11].

Two-photon lithography (TPL) is a microlithography technique based on two–photon absorption of laser radiation in a photoresist drop followed by polymerization and solidification of the exposed volume. The photoresist polymerized by two-photon absorption is localized near the focal spot of laser radiation. By moving the focal spot along a predetermined trajectory in the photoresist volume, it is possible to obtain three-dimensional microstructures with a resolution of down to 100 nm [12, 13].

The density and optical properties of structures manufactured by the TPL method depend on the printing parameters, for example, the laser power [14]. Therefore, by changing the laser power directly during printing, it is possible to change the optical properties of structures, setting the necessary profile of the refractive index gradient in any predetermined three-dimensional shape. At the moment, the use of TPL has been demonstrated for the fabrication of GRIN elements in porous silicon [15] and thin films [16]. Such methods, however, are limited in application, since porous structures are difficult to use in combination with optical waveguides, and thin films limit the size and shape of structures, in fact reducing three-dimensional lithography to two-dimensional.

In this work, we introduce the TPL technique for the manufacturing of three-dimensional microstructures with a continuous gradient of the refractive index. We improved the method of printing by two-photon lithography to add a gradient change of refractive index, manufactured test GRIN microstructures, and mapped the refractive index distribution in the fabricated microstructures.

FABRICATION OF EXPERIMENTAL SAMPLES

Figure 1 shows a schematic of an experimental TPL setup. A femtosecond TOptica FemtoFiber laser with a central wavelength of 780 nm and a pulse duration of 150 fs was used as a radiation source. Laser radiation goes through the acousto-optic modulator. After being deflected in the direction of the first diffraction maximum of the acousto-optic modulator, the laser beam

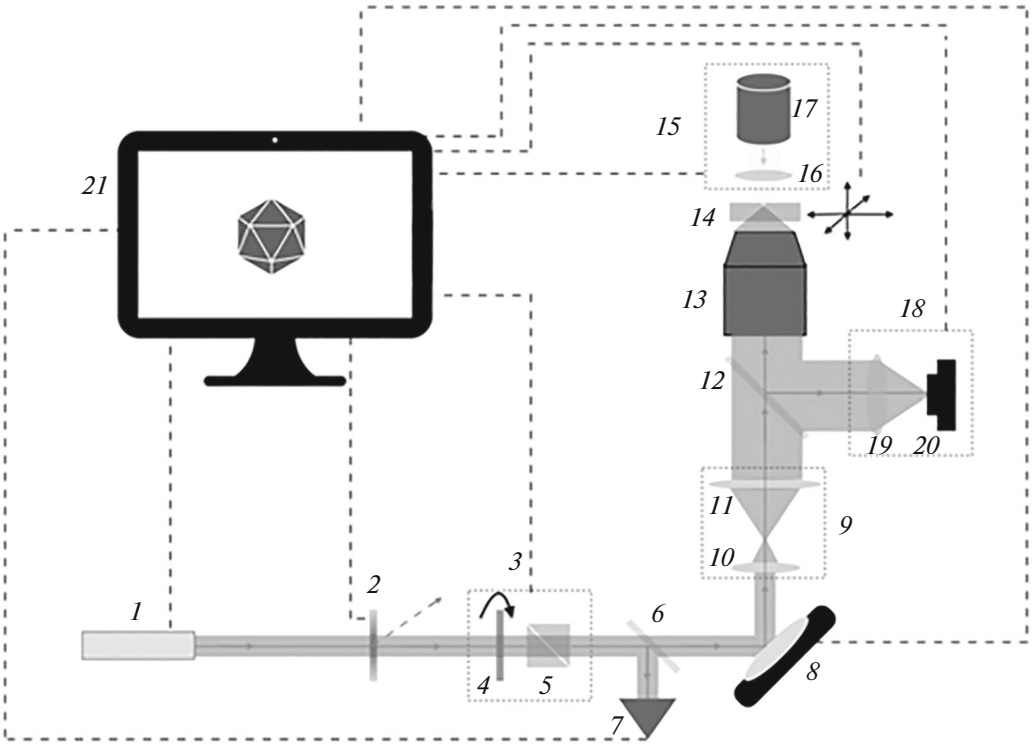

Fig. 1. Scheme of the two-photon lithography experimental setup: (*1*) laser; (*2*) acousto-optic modulator; (*3*) optical power control system; (*4*) half-wave phase plate; (*5*) Glan–Taylor prism; (*6*) beam splitter; (*7*) photodiode; (*8*) galvo mirror; (*9*) telescopic system of lenses (*10* and *11)*; (*12*) beam splitter; (*13*) lens; (*14*) substrate with photoresist; (*15*) illumination system; (*16*) collecting lens; (*17*) LED; (*18*) visualization system consisting of collecting lens (*19*) and camera (*20*); (*21*) computer.

passes through a power control system consisting of a half-wave plate and a Glan prism. Two-coordinate galvo mirror allows one to move the focal spot of laser radiation within the focal plane of the objective lens. The latter focuses the radiation inside the volume of the photoresist. The objective lens is mounted on a piezoelectric translator and can move in a direction perpendicular to the focal plane.

We have used the photoresist SZ2080 (IESL-Forth, Greece) [17] to print gradient microstructures. The photoresist is dropcasted on a glass substrate cleaned according to the following three-stage method: (1) mechanical cleaning of the surface followed by washing with acetone, isopropyl alcohol and distilled water, (2) chemical cleaning of the surface by holding the substrates in a "piranha" (a mixture of hydrogen peroxide with concentrated sulfuric acid in a ratio of 2:3) for 30 min, and (3) oxygen plasma treatment for 5 min. The liquid photoresist is dropcasted onto the substrate and then preprocessed in the oven at a temperature of 100°C for 60 min.

In the experimental setup, the reference power of the laser radiation is adjusted using a half-wave plate. In order to create a gradient optical microstructure, the working power relative to the reference power is changed directly during printing using an acousto-optic modulator, as this element allows the fast enough power modulation during the printing of microstructures. The laser power is variated by changing the control voltage on the modulator. The dependence of the modulator power on the applied voltage is nonlinear. To determine this, we have measured the calibration curve of the acousto-optic modulator. A voltage in the range 0 to 10 V was applied to the modulator in 0.1 V steps and the power of the transmitted radiation was measured at the first diffraction maximum using a photodiode. Measurements were performed for the input laser radiation with three powers: 80, 160 and 240 mW (Fig. 2). All curves coincide after being normalized to the maximum value of the transmitted power. This shows that the calibration curve of the acousto-optic modulator does not depend on the incoming laser power.

We have chosen the test sample to be in the shape of a rectangular parallelepiped with a square base of 25 × 25 μm and a height of 3 μm. The printing was carried out at the speeds of the laser beam in the range from 1000 to 3500 μm/s in increments of 1250 μm/s, and the working power in the range from 1 to 5 mW in increments of 1 mW.

The printed parallelepipeds had two different print power distribution profiles along one side of the square base: linear and Gaussian. These profiles allow to demonstrate the effectiveness of the printing

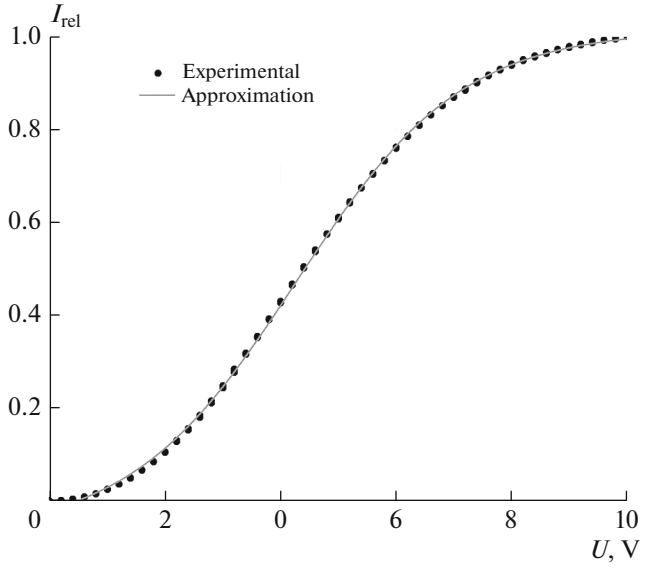

Fig. 2. Dots- the dependence of the relative intensity of the laser radiation (I/I_{max}), transmitted through the AOM on the voltage applied to the modulator. Curve: an approximation by the Boltzmann function.

method and to make a comparison with each other. The linear intensity dependence is implemented in such a way that the minimum intensity value is assigned to the minimum coordinate value for the structure, and the maximum intensity value is assigned to the maximum coordinate value. The Gaussian function is set by the coordinates of the peak, where the intensity value is maximum, and the line width is selected from the peak position, so that the radiation power at the edges of the figure is minimal. The parameters of the linear and Gaussian functions were changed to obtain samples with different refractive index gradients.

After TPL printing, the exposed samples were developed in methyl isobutyl ketone for 2 h, washed with distilled water and dried.

RESULTS

Figure 3a shows micrographs of the arrays of structures captured by an optical microscope. Each sample has been printed with its own set of printing parameters, such as the peak power and speed of the laser beam movement, as well as the function of changing the refractive index (relative laser power). It can be seen that part of the array is produced with sub-optimal parameters: either the structures are missing, that corresponds to an insufficient dose of absorbed radiation (below the polymerization threshold of the photoresist), or poor adhesion to the substrate; or the structures have characteristic inhomogeneities due to the too strong laser power, which leads to local heating and the polymer degradation. Figures 3b, 3c show arrays of microstructures with linear and Gaussian refractive index gradients, respectively. The circles mark the structures selected for subsequent measurements.

The spatial distribution of the refractive index was measured by optical coherence microscopy (OCM) [18]. This technique makes it possible to obtain three-dimensional images of translucent objects with micrometer resolution using the interference of the laser beam, reflected from the mirror, and the beam, reflected from the sample. Using OCM, one can determine the distribution of the reflectivity and the time delay of the beam in the sample, which gives information about the change in the refractive index [19]. The OCM method is successfully used to study the internal structure of integrated nanophotonics devices manufactured by two-photon lithography [20, 21]. OCM measurement revealed that the height of the manufactured microstructures is inhomoge-

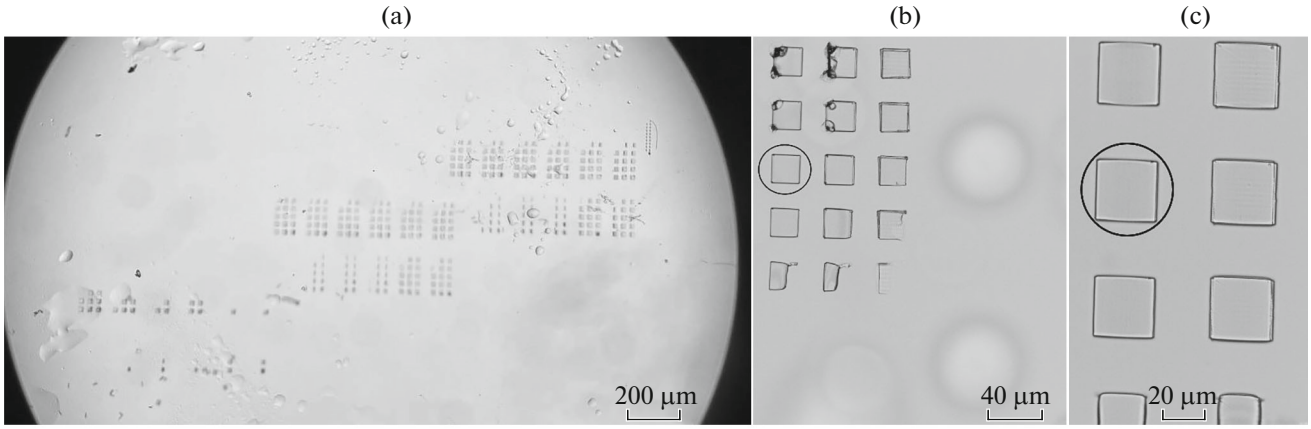

Fig. 3. Test samples micrographs captured by an optical microscope. The general arrangement of the printed structures on a glass substrate of structures (a) with a linear dependence of the laser radiation power during printing (b) and with a dependence described by the Gaussian function (c). The OCM measurements were carried out for circled structures.

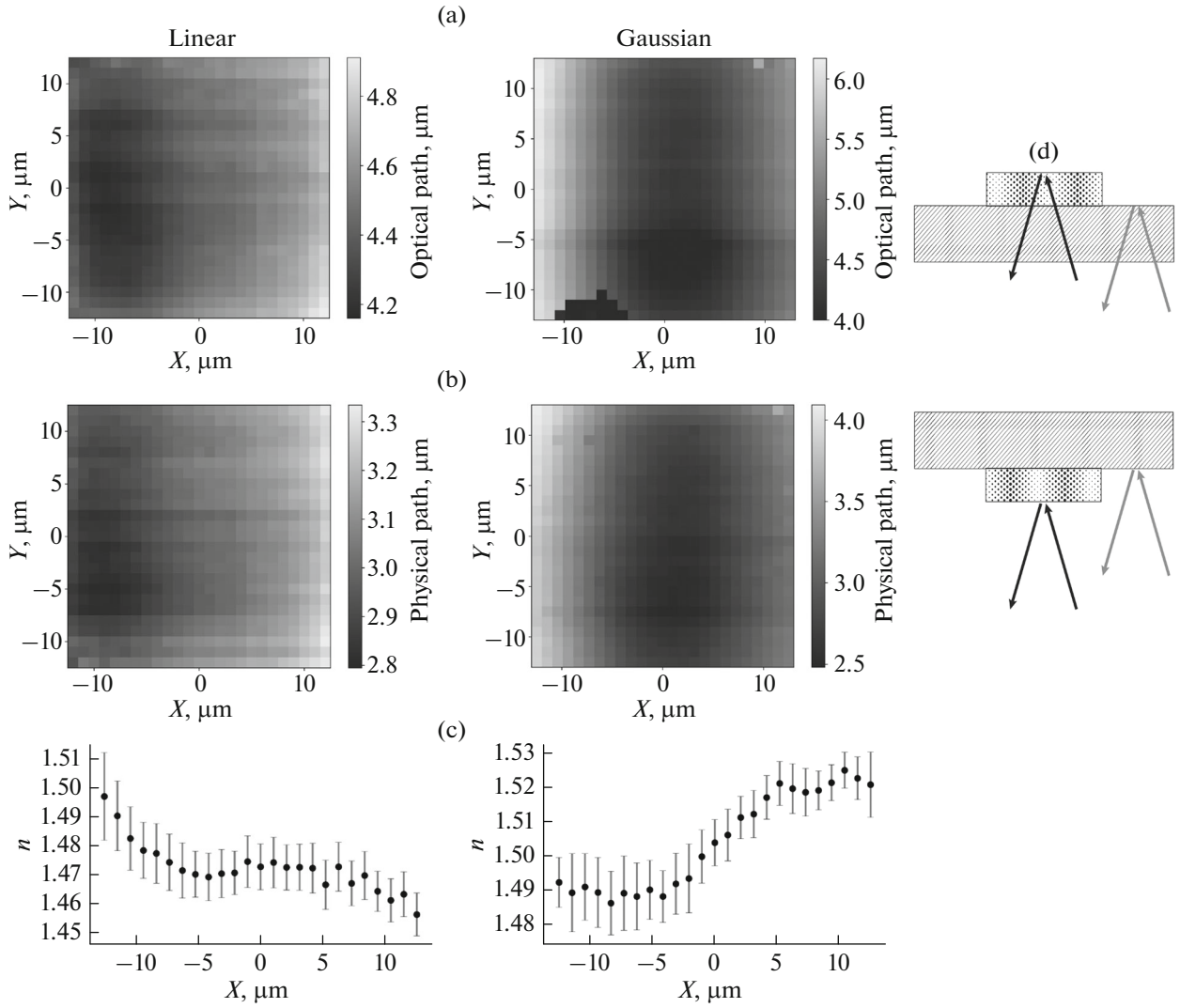

Fig. 4. Mapping of microstructures by the OCM method: two-dimensional graphs of the dependencies of the optical path on the coordinates in the microstructure (a); graphs of the dependencies of the physical path on the coordinates in the microstructure (b); dependencies of the refractive index averaged along the *Y* axis in the microstructure (c); schemes for obtaining optical and physical paths of the beam in the sample using OCM (d). Measurement of the optical (top) and physical (bottom) path of the signal (black arrows) beam in the sample compared to the reference beam (gray arrows).

neous and variates along with gradient of the optical refractive index. This finding was confirmed by atomic force microscopy [22], and the overall amplitude of height modulation of the structure was measured to be 440 nm. The inhomogeneity of the height of the manufactured structure arises due to the fact that the size of the polymerized volume of the photoresist depend on the power of the incident radiation, and this effect was taken into account when calculating the refractive index.

Measurements of gradient structures using the OCM method were carried out in two configurations. In the first configuration, the signal beam was passing first through the substrate, second the microstructure and then was reflected back from the upper boundary, while the reference beam was passing only through the substrate and then back after being reflected from the upper interface substrate-air. In the second configuration, the signal beam was immediately reflected from the structure, while the reference beam was reflected from the substrate. In both configurations, we compared the paths travelled by the signal and reference beams, as shown in Fig. 4d dark (signal beam) and light (reference beam) arrows, respectively. Since the reflection coefficient at the substrate-structure boundary is negligible, reflection from the structure-air boundary (air-structure) was observed in both cases. In the first configuration, the signal beam passed through the substrate and the structure and was reflected from the structure-air boundary, thus carrying information about the refractive index of the tra-

versed structure. In the second configuration, the signal beam passed only through the air and was reflected immediately at the air-structure boundary, and therefore did not carry information about the refractive index of the sample. This approach made it possible to measure both the optical path traversed by the signal beam inside the studied microstructures (Fig. 4a) and the physical path, that is, the height of the object (Fig. 4b). The ratio of these values gives the desired distribution of the refractive index in the manufactured structures, as it is shown in Fig. 4c. The obtained dependences qualitatively confirm that the TPL method allows fabrication of three-dimensional GRIN microstructures. The change in the refractive index inside the structure is $\Delta n = 0.03$. At the same time, the shape of the refractive index distribution itself differs from a given linear or Gaussian function. This discrepancy can be eliminated by conducting additional calibration studies. The absolute change in the refractive index turned out to be less than the corresponding values for gradient structures made in porous silicon [15], but twice as large as the value obtained in thin films [16].

CONCLUSIONS

The principal possibility of creating optical microstructures with a gradient refractive index using two-photon laser lithography is shown. Optical coherence microscopy showed that the refractive index in microstructures varies in the range $\Delta n = 0.03$. In the future we plan to develop the proposed method for creating three-dimensional optical elements with a gradient refractive index.

ACKNOWLEDGMENTS

The authors are grateful I.M. Antropov for measuring the height of the structure by atomic force microscopy.

FUNDING

The research was carried out within the framework of the Interdisciplinary Scientific and Educational School of Moscow University "Photonic and Quantum technologies. Digital Medicine". The work was supported by the RF Ministry of Science and Higher Education (grant no. 075-15-2021-1353).

CONFLICT OF INTEREST

The authors declare that they have no conflicts of interest.

REFERENCES

1. Reino, C., Perez, M., and Bao, C., *Gradient-Index Optics: Fundamentals and Applications*, Berlin: Springer, 2002.
2. Hwang, Y., Phillips, N., Dale, E.O., et al., *Opt. Express*, 2022, vol. 30, no. 8, p. 12294.
3. Reino, C., Perez, M.V., Bao, C., and Flores-Arias, T.M., *Laser Photonics Rev.*, 2008, vol. 2, no. 3, p. 203.
4. Kundal, S., Bhatnagar, A., and Sharma, R., *Optical and Wireless Technologies*, New York: Springer, 2022.
5. Pickering, M.A., Taylor, R.L., and Moore, D.T., *Appl. Opt.*, 1986, vol. 25, no. 19, p. 3364.
6. Ohmi, S., Sakai, H., Asahara, Y., et al., *Appl. Opt.*, 1988, vol. 27, no. 3, p. 496.
7. Sinai, P., *Appl. Opt.*, 1971, vol. 10, no. 1, p. 99.
8. Liu, J.H., Yang, P.C., and Chiu, Y.H., *J. Polym. Sci., Part A*, 2006, vol. 44, no. 20, p. 5933.
9. Liu, J.H. and Chiu, Y.H., *Opt. Lett.*, 2009, vol. 34, no. 9, p. 1393.
10. Mingareev, I., Kang, M., Truman, M., et al., *Opt. Laser Technol.*, 2020, vol. 126, p. 106058.
11. Dylla-Spears, R., Yee, T.D., Sasan, K., et al., *Sci. Adv.*, 2020, vol. 6, no. 47, p. eabc7429.
12. Mao, M., He, J., Li, X., et al., *Micromachines*, 2017, vol. 8, no. 4, p. 113.
13. Sharipova, M.I., Baluyan, T.G., Abrashitova, K.A., et al., *Opt. Mater. Express*, 2021, vol. 11, no. 2, p. 371.
14. Zhou, X., Hou, Y., and Lin, J., *AIP Adv.*, 2005, vol. 5, no. 3, p. 030701.
15. Ocier, R.C., Richards, C.A., Bacon-Brown, D.A., et al., *Light Sci. Appl.*, 2020, vol. 9, p. 196.
16. Žukauskas, A., Matulaitienė, I., Paipulas, D., et al., *Laser Photonics Rev.*, 2015, vol. 9, no. 6, p. 706.
17. Pertoldi, L., Zega, V., Comi, C., and Osellame, R., *J. Appl. Phys.*, 2020, vol. 128, no. 17.
18. Drexler, W. and Fujimoto, J.G., *Optical Coherence Tomography: Technology and Applications*, New York: Springer, 2008.
19. Sirotin, M.A., Romodina, M.N., Lyubin, E.V., et al., *Biomed. Opt. Express*, 2022, vol. 13, no. 1, p. 14.
20. Safronov, K.R., Gulkin, D.N., Antropov, I.M., et al., *ACS Nano*, 2020, vol. 14, no. 8, p. 10428.
21. Safronov, K.R., Bessonov, V.O., Akhremenkov, D.V., et al., *Laser Photonics Rev.*, 2022, vol. 16, no. 4, p. 2100542.
22. Giessibl, F.J., *Rev. Mod. Phys.*, 2003, vol. 75, no. 3, p. 949.